iScience

CellPress
OPEN ACCESS

Article

Utilization of potato starch suspension for MR-microimaging in *ex vivo* mouse embryos

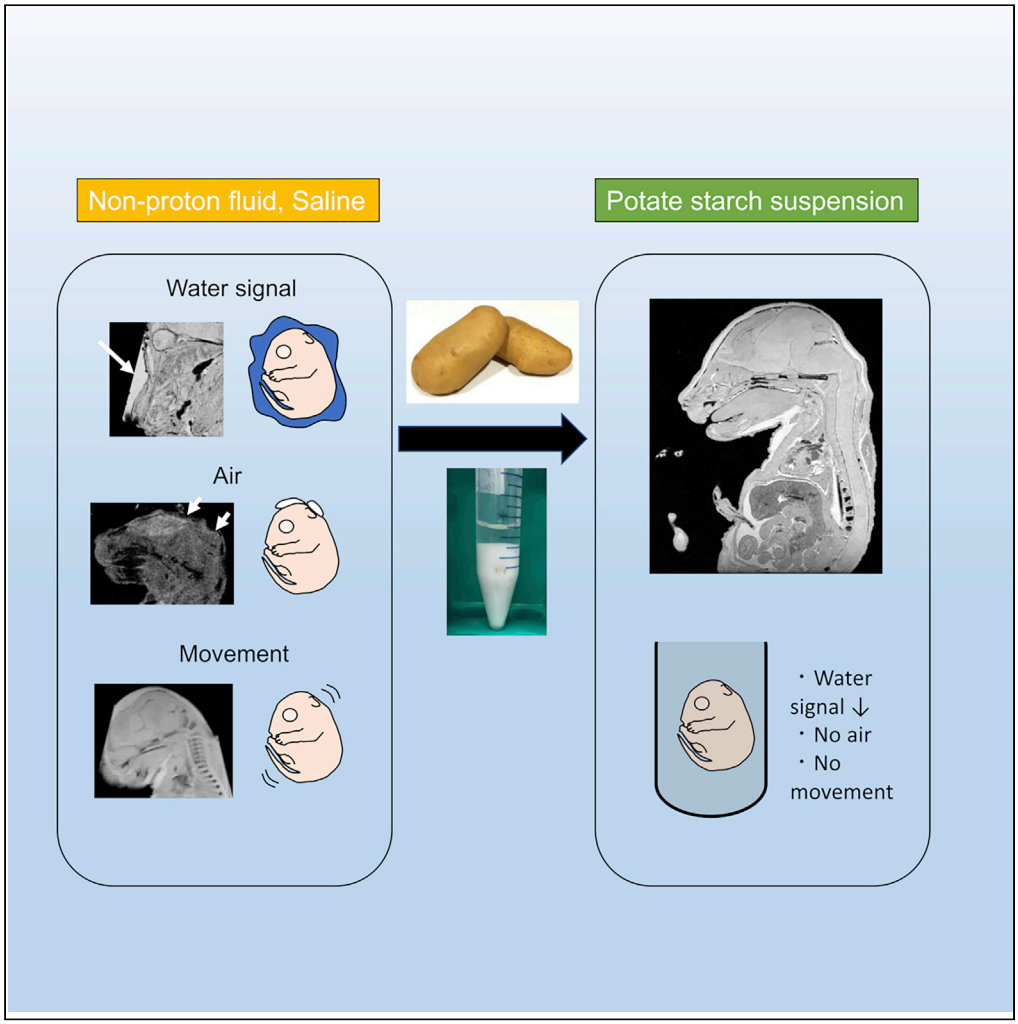

Tomokazu Tsurugizawa, Takuma Kumamoto, Yoshichika Yoshioka

t-tsurugizawa@aist.go.jp (T.T.)
yoshioka@fbs.osaka-u.ac.jp (Y.Y.)

Highlights

Potato starch suspension shows a low T1 and T2 signal intensity

Potato starch suspension strongly prevents the movement of the embryo

Potato starch suspension is useful for *ex vivo* MR microimaging of mouse embryos

Tsurugizawa et al., iScience 25, 105694
December 22, 2022
https://doi.org/10.1016/j.isci.2022.105694

iScience

CellPress
OPEN ACCESS

Article

Utilization of potato starch suspension for MR-microimaging in *ex vivo* mouse embryos

Tomokazu Tsurugizawa,[1,2,3,4,5,7,*] Takuma Kumamoto,[6] and Yoshichika Yoshioka[4,5,*]

SUMMARY

Magnetic resonance (MR) microimaging of the mouse embryo is a promising tool to noninvasively investigate the microstructure of the brain of a developing mouse. The proton-free fluid is used for the liquid surrounding the specimen in MR microimaging, but the potential issue of image quality remains due to the air bubbles on the specimen and the retained water proton in the curvature of the embryo. Furthermore, the specimen may move during the scanning, resulting in motion artifact. Here, we developed the new concept of the *ex vivo* microimaging protocol with the robust method using the potato starch-containing biological polymers. Potato starch suspension with PBS significantly reduced T1 and T2 signal intensity of the suspension and strongly suppressed the motion of the embryo. Furthermore, potato starch-PBS suspension is stable for long-time scanning at room temperature. These results indicate the utility of potato starch suspension for MR microimaging in mouse embryos.

INTRODUCTION

Magnetic resonance imaging (MRI) is a promising tool for noninvasive medical imaging in animal models as well as humans.[1–3] Microimaging of the mouse embryo, which is investigated to clarify the developmental mechanism of the brain, requires *ex vivo* ultrahigh-resolution imaging[4,5] to overcome limitations, such as the scanning time, body movement, and physiological artifact of *in vivo* brain.[4–7] The *ex vivo* MRI, with high resolution and high signal-to-noise ratio, enables us to investigate the fiber network, as well as the whole brain structure, without cutting the brain, such as immunohistochemistry.[8,9] The recent progress of the database of histology and high-resolution MRI of *ex vivo* mouse embryo enables us to compare them directly.[10,11] Importantly, MRI is available to investigate the microstructure of the human embryo *in utero* noninvasively.[12] The detailed microstructural comparison between histology and MRI could be helpful to understand the human embryo brain.

The microstructure of the mouse embryo has also been imaged using computed tomography and the mouse embryo was immersed in the 1% (w/v) agarose to suppress motion artifacts.[13,14] However, the agarose gel contains water protons, which have strong signals as a background in T1- and T2-weighted images,[15] and it is thus not available to fix the embryo on MRI. Embryos are generally immersed in liquid in *ex vivo* MRI to avoid susceptibility artifacts arising from tissue-air interfaces, and proton-free fluids, such as Fluorinert and Fomblin, have been widely used as they remove background signals and match tissue susceptibility.[16–18] However, the potential issue of image quality remains due to the air bubbles on the edge of the specimen, as well as the motion.[19] Additionally, if the water surrounding the tissue is not perfectly removed, the water proton signal remains on the surface of the tissue and disturbs the tissue masking.

The present study hypothesized that potato starch (PS) suspension with PBS (PS-PBS) is useful as a surrounding liquid for *ex vivo* MRI by suppressing the background signal intensity arising from water proton and the movement of the specimen. PS is one of the most abundant natural biological polymers, including amylose and amylopectin[20]; thus, it has been used in various fields, such as chemicals, foods, and medicine.[21] In addition to the chemical characteristics, shear thickening (also terms as dilatant), which suddenly increases the viscosity of the suspension above rapid stress, exists in PS suspension.[22] This effect is expected to suppress the motion of the embryo caused by the vibration of gradient coils during scanning. Furthermore, PS not only shortens the T2 of water protons by interfering spin-spin interaction of water protons but also suppresses the signal intensity of water protons.[23] At room temperature, PS suspension is

[1]Human Informatics and Interaction Research Institute, National Institute of Advanced Industrial Science and Technology (AIST), 1-1-1 Higashi, Tsukuba 305-8568, Japan

[2]Faculty of Engineering, Information and Systems, University of Tsukuba, Tsukuba 305-8573, Japan

[3]Jikei University School of Medicine, 3-25-8 Nishishinbashi, Tokyo 105-8461, Japan

[4]Graduate School of Frontier Biosciences, Osaka University, Suita 565-0871, Japan

[5]Center for Information and Neural Networks (CiNet), Osaka University and National Institute of Information and Communications Technology (NICT), Suita 565-0871, Japan

[6]Developmental Neuroscience Project, Department of Brain & Neurosciences, Tokyo Metropolitan Institute of Medical Science, Tokyo 156-8506, Japan

[7]Lead contact

*Correspondence: t-tsurugizawa@aist.go.jp (T.T.), yoshioka@fbs.osaka-u.ac.jp (Y.Y.)

https://doi.org/10.1016/j.isci.2022.105694

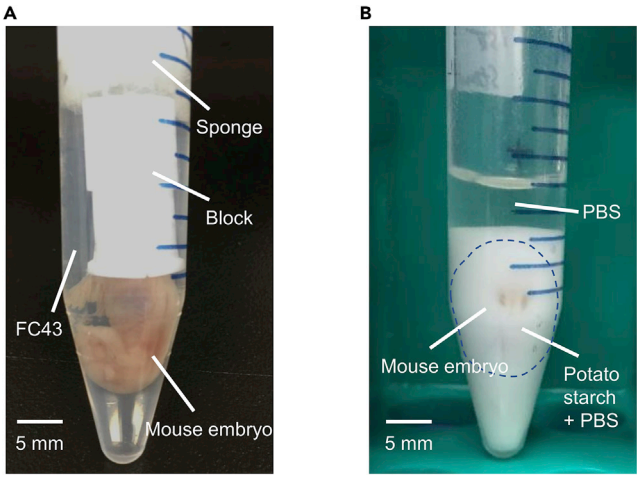

Figure 1. Representative photos of mouse embryo with FC43 or PS-PBS

(A) A photo of a representative mouse with FC43. The sponge and the plastic block were used to prevent the motion artifact of the mouse embryo.

(B) A photo of a representative mouse with PS-PBS. The dotted line indicates the position of the embryo. Scale bar indicates 5 mm. All of the data were obtained from one male mouse.

stable during long-time MRI scanning; thus, these features are consistent during the long-time scan. Here, we compared PBS (containing water proton), FC43 (proton-free fluid), and PS-PBS to assess the hypothesis. We also assessed the utility of PS suspension with gadolinium (Gd), which is a commonly used contrast agent, because *ex vivo* MRI sometimes uses the specimen accumulated with Gd.

RESULTS

Microimaging with Gd-PS-PBS and potential artifacts with FC43

During the MRI scanning of the mouse embryo with PBS, PBS containing Gd (Gd-PBS), or FC43, the whole body of the embryo was fixed using the sponge and plastic block (Figure 1A), while mouse embryo with PS-PBS and PS-PBS containing Gd (Gd-PS-PBS) did not require the materials (Figure 1B). The representative ultrahigh-resolution image of the embryo with Gd-PS-PBS provides detailed information on tissue microstructure (Figure 2A and Video S1). Remarkably, the risk of the artifacts shown below (Figures 2B–2D) was excluded when using PS-PBS or Gd-PS-PBS. FC43 is available for *ex vivo* MRI due to its no signal intensity; however, the researchers encounter some risks of artifacts in MR microimaging. Even though fixation of the embryo and exchange of water to non-proton liquid was carefully performed, the susceptibility artifacts sometimes occur. Here, we presented the three types of artifacts in microimaging. First is a high signal intensity on the tissue boundary by retained water proton (Figure 2B). Second, an air bubble sticks on the surface of the embryo and induces severe artifacts on the embryo. The image quality of the entire brain is affected by air bubbles because the volume in the embryo is smaller than in the adult brain (Figure 2C). The third is the motion artifact (Figure 2D). The outside air bubbles can often be removed by vacuum when Fluorinert or PBS is used as immersion fluid. It is more problem for PBS on tissue boundary as shown in Figure 2B because it is sometimes difficult to remove it. Soft materials were used to suppress the motion of the embryo without deforming the head (Figure 1). However, slight movements resulted to blur images in high-resolution imaging of the embryo. The movement of the embryo with PS-PBS during the scanning of T1- and T2-weighted image was assessed (Figure S1). The translation of the embryo during 10 repetitive scanning of T1- and T2-weighted images was smaller than 1/4 of the voxel size (0.078 mm). The rotation of the embryo was extremely small. The averaged image did not show the motion artifact. These results support the suppression of the motion of the embryo during the scanning. The movement of the embryo with PBS could not be measured because it was difficult to identify the whole body of the embryo correctly due to similar signal intensity between the embryo and PBS. FC43 has a higher specific gravity than the specimen, so the embryo will float without material to prevent the motion of the embryo. The movement of the embryo with FC43 was therefore measured with the sponge and the block (Figure S2). Remarkably, the movement of the embryo with PS-PBS was within the same range as that of the sponge and the block in FC43.

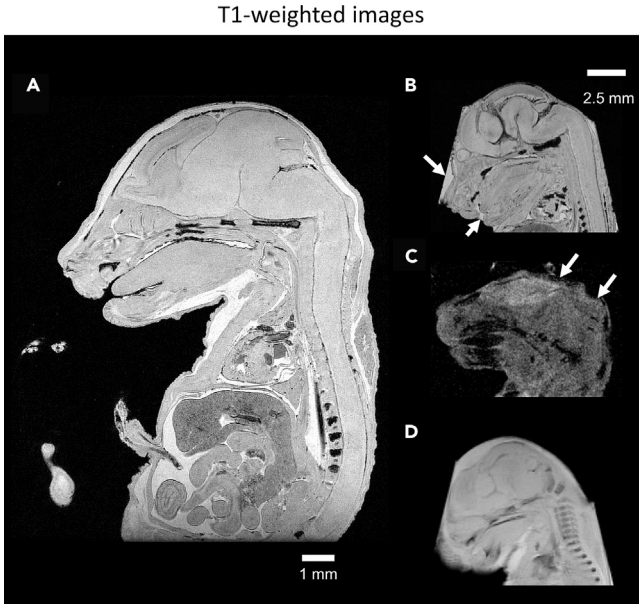

Figure 2. Representativeimages of microimaging of an embryo with Gd-PS-PBS and artifacts of an embryo with FC43

(A) Ultrahigh-resolution image of mouse embryo with Gd-PS-PBS. Scale bar indicates 1 mm.

(B) Retained water on the surface of the tissue shows high signal intensity (arrow).

(C) Susceptibility artifact caused by air bubbles on tissue-air interfaces at the tissue edges (arrow) in image.

(D) The blurred edge of the image is caused by tissue movements. The images in (B–D) were obtained using FC43. All images are T1 images. Scale bar indicates 1 mm. All of the data were obtained from one male mouse.

T1 and T2 relaxation curves among the solutions

The T1 and T2 relaxation of PBS, Gd-PBS, PS powder, PS-PBS, and Gd-PS-PBS were compared (Figure 3). The T1-weighted signals of PS powder, PS-PBS, and Gd-PS-PBS were lower than those of PBS and Gd-PBS (Figure 3A). The T1 relaxation curves showed that the signal intensity of PS powder, PS-PBS, and Gd-PS-PBS was higher than that of the background, but they were extremely lower than that of PBS and Gd-PBS when longitudinal magnetization was recovered at repetition time (TR) of 5,000 ms (Figure 3B). As the Gd-PBS reduces the T1 relaxation time of water proton, Gd-PBS induced the earlier recovery of the longitudinal signal rather than PBS only (Figure 3B and Table 1). The T1 relaxation time in PS powder, PS-PBS, and Gd-PS-PBS could not be calculated because of their low signal intensity throughout all TRs. The T2 relaxation curve was also investigated using long echo time (TEs) and short TEs in the same solutions (Figures 3C and 3D, and Table 1), which showed that the signal intensity of PS powder, PS-PBS, and Gd-PS-PBS was higher than that of the background, but their signal intensity was extremely lower than that of PBS and Gd-PBS. As the Gd reduced the T2 relaxation time of water proton (Table 1), Gd induced the earlier decrease of the transverse signal intensity of Gd-PBS rather than that of PBS. The T2 relaxation time in PS powder, PS-PBS, and Gd-PS-PBS could not be calculated because of their low signal intensity and rapid reduction of the T2 relaxation curve (Figure 3D and Table 1).

The comparison of background signals in T1- and T2-weighted embryo images

T1-weighted embryo images were acquired to compare the background signals of PBS, Gd-PBS, FC43, PS-PBS, and Gd-PS-PBS using the same embryo (Figures 4 and 5). The T1-weighted signal intensity of PBS was similar to that of the body of the embryo (Figure 4A). Contrarily, T1-weighted images of mouse embryos with FC43 and with PS-PBS showed that the background signal intensity was significantly less than that of the embryo (Figures 4B and 4C). The T1-weighted image with a Gd-contrast agent showed a better brain microstructure contrast (Figures 4D–4F). The background signal of Gd-PBS was similar to that of the embryo brain, while the background signals of FC43 and Gd-PS-PBS showed low signals compared with that of the embryo (Figures 4E and 4F).

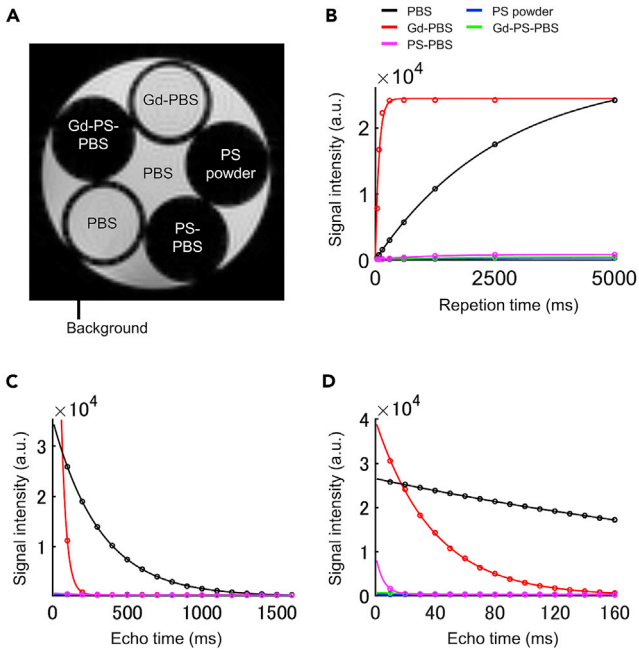

Figure 3. T1 and T2 relaxation time

(A) T2-weighted image of the solution (n = 1).

(B) T1 relaxation, (C) T2 relaxation of each solution with long TEs, and (D) T2 relaxation of each solution with short TEs. The color lines indicate PBS (black), Gd-PBS (red), PS powder (blue), PS-PBS (magenta), and Gd-PS-PBS (green), respectively (n = 1 for each condition).

The utility of PS-PBS for T2-weighted images was also assessed (Figure 5). The signal intensity of PBS in the T2-weighted image was similar to that in the body of the mouse embryo (Figure 5A). Contrarily, the T2-weighted image of mouse embryo with FC43 or with PS-PBS showed that their signal intensity was significantly less than that of the embryo (Figures 5B and 5C). The T2-weighted image with a Gd-contrast agent was also investigated (Figures 5D–5F). Gd induced an ameliorated contrast in the brain. The background signals of FC43 or Gd-PS-PBS showed low signals compared with that of the embryo (Figures 5E and 5F). The averaged signal intensity between surrounding liquid and the brain tissue of the embryo was investigated (Table 2). The signal intensities of PS-PBS and Gd-PS-PBS were comparable to FC43 and smaller than those of embryonic tissue. In contrast, the signal intensities of PBS and Gd-PBS were comparable to those of embryonic tissue. The materials for fixing the embryo may cause missing signals near the material and deformation of the specimen (Figures 5A and 5B). The part of the specimen in contact with the wall of the tube is deformed a little (Figures 5A, 5B, 5D, and 5E), and the small bent of the embryo body was observed in Figure 5D due to the force for fixation of the specimen, while the deformation and missing signals were not observed with PS-PBS and Gd-PS-PBS.

Table 1. Averaged signal intensity, T1 and T2 relaxation time

	T1-weighted image		T2w-weighted image	
Solution	Signal intensity at TR = 5000 ms	T1 (ms)	Signal intensity at TE = 10 ms	T2 (ms)
PBS	2.418×10^4	2622	2.579×10^4	167.0
Gd-PBS	2.414×10^4	76.17	3.057×10^4	38.64
PS	383.3	–	368.9	–
PS-PBS	866.0	–	1664	–
Gd-PS-PBS	511.7	–	668.9	–
Background	176.8	–	92.73	–

-: T1 relaxation times could not be calculated due to the low signal. N = 1 for each condition.

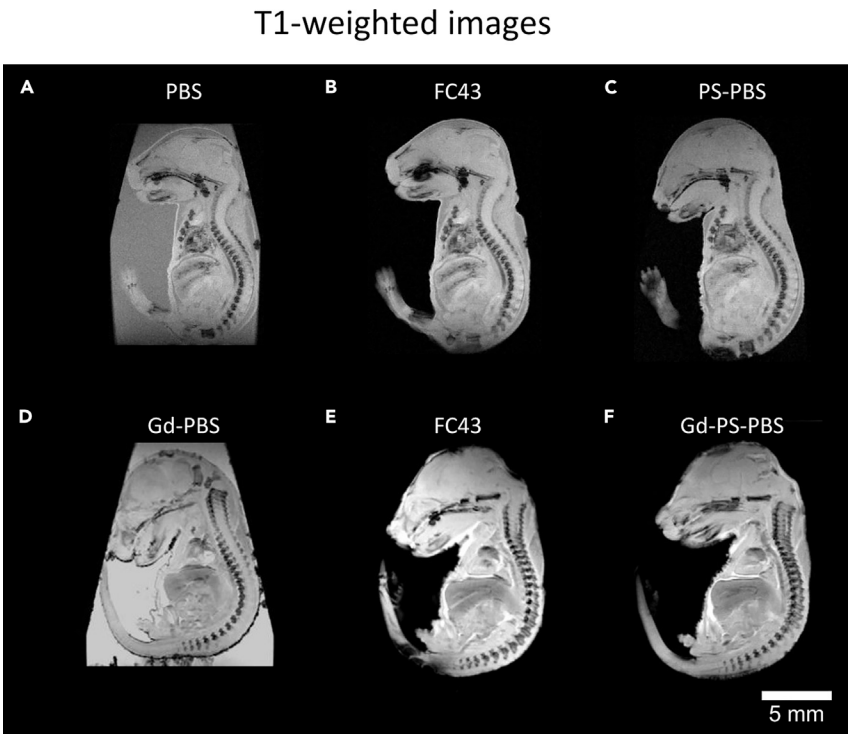

Figure 4. T1-weighted images of the mouse embryo

(A–C) T1-weighted gradient-echo images of mouse embryo immersed in (A) PBS, (B) FC43, and (C) PS-PBS (n = 1 for each condition). (D-F) T1-weighted gradient-echo images of mouse embryo with gadolinium immersed in (D) Gd-PBS, (E) FC43, and (F) Gd-PS-PBS (n = 1 for each condition). Scale bar indicates 5 mm.

DISCUSSION

The present study showed the use of PS-PBS and Gd-PS-PBS for the MR microimaging study of mouse embryos. The size of the mouse embryo's brain is extremely smaller than that of the adult mouse; thus, the entire image quality is heavily influenced by artifact. The main artifacts that bother us are (1) background noise, (2) susceptibility artifacts arising from air bubbles, and (3) motion artifacts (Figures 2B–2D). Our study results demonstrated the utility of PS-PBS and Gd-PS-PBS in an *ex vivo* micro-MRI study beyond these artifacts. The concept of the surrounding liquid is so far the water proton signal removal, but the risk of body movement and air bubbles remained. Contrary, this study showed the new strategy of using biological polymers as a surrounding liquid that suppresses the T1-/T2-weighted signals of water proton and keeps air soluble in the suspension at room temperature for a long time. PS is insoluble with water but is stably diffused in water. It is never gelatinized nor swelled at room temperature. Therefore, it is unlikely to dehydrate the specimen or conversely increase the water content of the specimen, and it is unlikely to penetrate the tissue. Also, potato starch particles settle slowly and do not compress the tissue. Tissue deformation should not thus be considered. Figure S3 shows no significant difference in the entire volume of the mouse, which was approximately 672 mm^2 between FC43 and PS-PBS. Mouse embryos can also be easily moved from PS suspension after the experiment, and the PS suspension is reusable. Essentially, the embryo can be maintained in the suspension composed of PS and the same solvent in which they were preserved following fixation, such as PBS or Gd-PBS. In contrast, proton-free fluids require careful water proton-free fluid exchange. Additionally, dedicated materials are required to fix the position of the specimen because proton-free fluid has a high specific gravity (Figure 1). During the long-time scanning, the water in the tissue will gradually be exchanged for FC43 due to the osmotic pressure, but it does not leave the tissue when using PS-PBS suspension. Additionally, we confirmed that PS-PBS and Gd-PS-PBS were stable as the suspension of PS for at least three months, indicating the availability of long-time scanning. The previous study also reports the stability of the suspension.[24] Therefore, these PS characteristics indicate the alternative utility of PS suspension in *ex vivo* micro-MRI compared with conventional non-proton fluid.

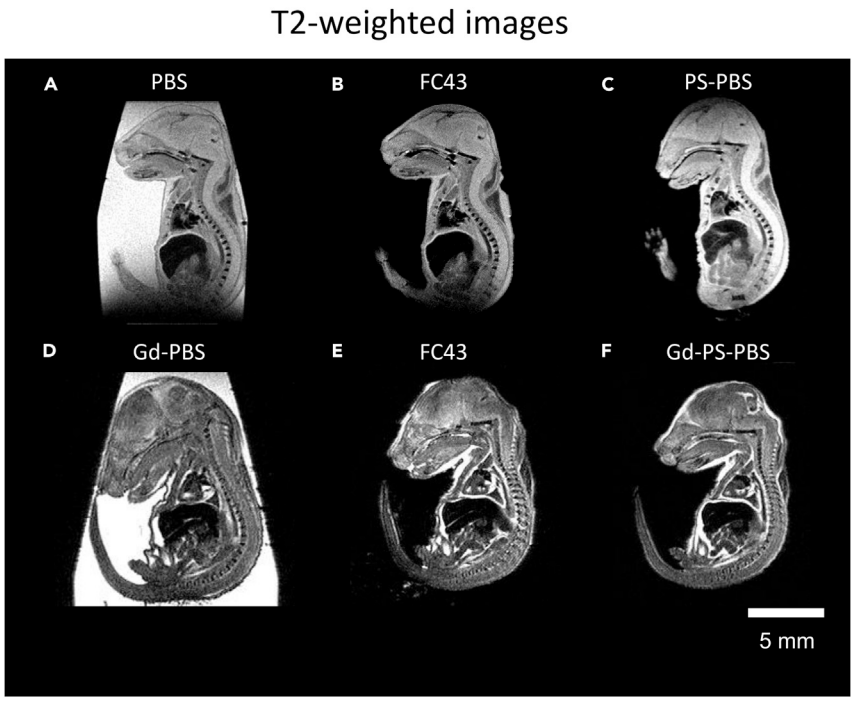

Figure 5. T2-weighted images of the mouse embryo

(A–C) T2-weighted spin-echo images of mouse embryo immersed in (A) PBS, (B) FC43, and (C) PS-PBS (n = 1 for each condition).

(D–F) T2-weighted gradient-echo images of mouse embryo with gadolinium immersed in (D) Gd-PBS, (E) FC43, and (F) Gd-PS-PBS (n = 1 for each condition). Scale bar indicates 5 mm.

The T1- and T2-weighted signals of PS-PBS were lower than those of PBS (Figure 3). Luo et al. investigated the effect of adding PS into the hairtail surimi gel. The PS dose-dependently induced not only the shortening of spin-spin relaxation time of gel but also the reduced signal intensity. The fraction with the shortest T2 in PS suspension is related to non-exchangeable protons of CH in both the amylopectin and amylose.[25] Additionally, they reported reduced water mobility in PS suspension, suggesting the metastasis of free water to bound water on the microstructure composed of amylose and amylopectin.[26] This metastasis of free water to bound water in PS-PBS may contribute to low signal intensity in the T1-weighted image. A previous NMR study measured proton vertical relaxation time (T2) and longitudinal relaxation time (T1) of PS hydrate at room temperature.[27] T1 and T2 relaxation time or water proton is 49 and 0.264 ms at 10.6% water content of PS suspension. These data indicate the low signal intensity of PS-PBS within the time range of TE and TR, which is an appropriate time for the embryo in T1- and T2-weighted images.

The air bubble that dissolved in the PBS sometimes sticks to the small unevenness of the embryo when using the proton-free fluid or PBS as the surrounding liquid, resulting in the susceptibility artifact on the tissue edge. This susceptibility artifact is sometimes observed with FC43 in a long-time scanning (Figure 2C). The long-time scan alters the temperature and pressure of the surrounding liquid, making the bubbles grow bigger, resulting in the air bubble sticking to the specimen surface. In brain imaging, the possible solution is scanning with the skull to keep the brain far from the air bubble on the boundary.[28,29] However, this method is impossible in mouse embryo imaging due to the thinner and immature skull. Another solution is to immerse the MRI-compatible container in water or formalin, place the brain inside, and gently agitate to remove small surface bubbles.[19] Otherwise, using the degassed liquid is also effective.[30,31] Careful removal of air bubbles, such as by the vacuum, can reduce the frequency of air bubbles, but this process sometimes takes time to completely remove the bubble. The merit of PS suspension is that it does not require degassing, which allows more efficient preparation of the samples than using FC43 and PBS. Remarkably, the artifact caused by the air bubble was not observed in long-time scanning of the embryo when using Gd-PS-PBS (Figure 2A). The mechanism of air bubble suppression remained unclear but possibly explained by the

Table 2. Averaged signal intensity of surrounding liquid and the tissue of the embryo

	T1-weighted image		T2w-weighted image	
Solution	Surrounding liquid	embryo	Surrounding liquid	embryo
PBS	1.773×10^4	2.066×10^4	1.742×10^4	1.095×10^4
Gd-PBS	5.793×10^4	3.876×10^4	1.345×10^4	4731
FC43	1011	2.222×10^4	884	1.206×10^4
FC43 with Gd-embryo	922	4.461×10^4	993	8811
PS-PBS	1506	1.727×10^4	1185	1.094×10^4
Gd-PS-PBS	1126	3.458×10^4	993	7291

N = 1 for each condition.

chemical characteristic of PS-PBS. The PS-PBS has a micro-architecture composed of amylose and amylopectin, and the interaction between polymers and water may stabilize the air solved in the liquid.[32]

The embryo with PS-PBS or Gd-PS-PBS did not move during long-time scanning. This phenomenon could be explained by shear thickening. Non-Brownian suspensions of hard frictional particles immersed in a viscous fluid are Newtonian.[22] The repulsive force prevents the grains from coming into contact at a small shear rate. Thus, the suspension flows easily as if particles were frictionless. In contrast, at the large shear rate, the repulsive force is overcome by the hydrodynamic forces so that particles are pressed into frictional contacts. The effect of shear thickening on embryo vibration during scanning has not been investigated. This hypothesis will be assessed in future studies.

In conclusion, the mixed suspension of PS and PBS can solve the issue of MR microimaging of the brain of the embryo, such as air bubbles, specimen motion, and proton signals of the surrounding fluid. These results give the new strategy of surrounding fluid for *ex vivo* micro-MRI. This effect is possibly due to the chemical structure of PS-PBS. In addition to the PS, a starch-like additive such as corn starch suspension that involves the amylose and amylopectin shows the property of dilatant liquid; thus, another starch suspension should be investigated in the future.

Limitations of the study

We could not calculate the T1 and T2 relaxation times of PS powder, PS-PBS, and Gd-PS-PBS because of low signal intensity and short relaxation time. Instead, we discussed with the previous study that reported that T1 and T2 relaxation time of water proton in PS suspension is 49 and 0.264 ms, respectively.[27]

In addition to the PS, a starch-like additive such as corn starch suspension that involves the amylose and amylopectin shows the property of dilatant liquid, but another starch suspension was not investigated in this study. Thus, it should be investigated in the future.

STAR★METHODS

Detailed methods are provided in the online version of this paper and include the following:

- KEY RESOURCES TABLE
- RESOURCE AVAILABILITY
  - Lead contact
  - Materials availability
  - Data and code availability
- EXPERIMENTAL MODELS AND SUBJECT DETAILS
  - Animals
- METHOD DETAILS
  - Sample preparation
  - T1 and T2 relaxation time measurement
  - T1-and T2-weighted images of mouse embryos
  - Image processing
- QUANTIFICATION AND STATISTICAL ANALYSES

SUPPLEMENTAL INFORMATION

Supplemental information can be found online at https://doi.org/10.1016/j.isci.2022.105694.

ACKNOWLEDGMENTS

This research in the laboratory of T.T. was supported by Grant-in-Aid for Challenging Research (Exploratory) in Japan (grant number 21K19464) and by a Grant-in-Aid for Research Activity Start-up in Japan (grant number 20K22698). The study of Y.Y. was supported in part by Grant-in-Aid for Scientific Research (A) (grant number 16H01849) from the Ministry of Education, Culture, Sports, Science, and Technology of Japan. The study of T.K. was supported by Grant-in-Aid for Research Activity Start-up in Japan, grant number 20K22665, a Leading Initiative for Excellent Young Researchers (LEADER), grant number 2020L0019, and the Takeda Science Foundation, Japan.

AUTHOR CONTRIBUTIONS

T.T. and Y.Y. directed the project. T.T. and Y.Y. established the methodology of MRI experiment and performed the experiment. T.K. prepared the *ex vivo* mouse embryo. T.T. analyzed the data. T.T., Y.Y., and T.K. wrote and revised the manuscript.

DECLARATION OF INTERESTS

The authors declare no competing interests.

INCLUSION AND DIVERSITY

We support inclusive, diverse, and equitable conduct of research.

Received: May 25, 2022
Revised: July 31, 2022
Accepted: November 24, 2022
Published: December 22, 2022

REFERENCES

1. Mandino, F., Cerri, D.H., Garin, C.M., Straathof, M., van Tilborg, G.A.F., Chakravarty, M.M., Dhenain, M., Dijkhuizen, R.M., Gozzi, A., Hess, A., et al. (2019). Animal functional magnetic resonance imaging: Trends and Path toward Standardization. Front. Neuroinform. *13*, 78. https://doi.org/10.3389/fninf.2019.00078.

2. Denic, A., Macura, S.I., Mishra, P., Gamez, J.D., Rodriguez, M., and Pirko, I. (2011). MRI in rodent models of brain disorders. Neurotherapeutics *8*, 3–18. https://doi.org/10.1007/s13311-010-0002-4.

3. Edelman, R.R. (2014). The history of MR imaging as seen through the pages of radiology. Radiology *273*, S181–S200. https://doi.org/10.1148/radiol.14140706.

4. Wu, D., and Zhang, J. (2016). Recent progress in magnetic resonance imaging of the embryonic and neonatal mouse brain. Front. Neuroanat. *10*, 18. https://doi.org/10.3389/fnana.2016.00018.

5. Kumamoto, T., and Tsurugizawa, T. (2021). Potential of multiscale astrocyte imaging for revealing mechanisms underlying neurodevelopmental disorders. Int. J. Mol. Sci. *22*, 10312. https://doi.org/10.3390/ijms221910312.

6. Oguz, I., Yaxley, R., Budin, F., Hoogstoel, M., Lee, J., Maltbie, E., Liu, W., and Crews, F.T. (2013). Comparison of magnetic resonance imaging in live vs. post mortem rat brains. PLoS One *8*, e71027. https://doi.org/10.1371/journal.pone.0071027.

7. Roebroeck, A., Miller, K.L., and Aggarwal, M. (2019). Ex vivo diffusion MRI of the human brain: Technical challenges and recent advances. NMR Biomed. *32*, e3941. https://doi.org/10.1002/nbm.3941.

8. Yon, M., Bao, Q., Chitrit, O.J., Henriques, R.N., Shemesh, N., and Frydman, L. (2020). High-resolution 3D in vivo brain diffusion tensor imaging at ultrahigh fields: following maturation on juvenile and adult mice. Front. Neurosci. *14*, 590900. https://doi.org/10.3389/fnins.2020.590900.

9. Edlow, B.L., Mareyam, A., Horn, A., Polimeni, J.R., Witzel, T., Tisdall, M.D., Augustinack, J.C., Stockmann, J.P., Diamond, B.R., Stevens, A., et al. (2019). 7 Tesla MRI of the ex vivo human brain at 100 micron resolution. Sci. Data *6*, 244. https://doi.org/10.1038/s41597-019-0254-8.

10. Petiet, A.E., Kaufman, M.H., Goddeeris, M.M., Brandenburg, J., Elmore, S.A., and Johnson, G.A. (2008). High-resolution magnetic resonance histology of the embryonic and neonatal mouse: a 4D atlas and morphologic database. Proc. Natl. Acad. Sci. USA *105*, 12331–12336. https://doi.org/10.1073/pnas.0805747105.

11. Chen, A., Liao, S., Cheng, M., Ma, K., Wu, L., Lai, Y., Qiu, X., Yang, J., Xu, J., Hao, S., et al. (2022). Spatiotemporal transcriptomic atlas of mouse organogenesis using DNA nanoball-patterned arrays. Cell *185*, 1777–1792.e21. https://doi.org/10.1016/j.cell.2022.04.003.

12. Grossman, R., Hoffman, C., Mardor, Y., and Biegon, A. (2006). Quantitative MRI measurements of human fetal brain development in utero. Neuroimage *33*, 463–470. https://doi.org/10.1016/j.neuroimage.2006.07.005.

13. Cole, J.M., Symes, D.R., Lopes, N.C., Wood, J.C., Poder, K., Alatabi, S., Botchway, S.W., Foster, P.S., Gratton, S., Johnson, S., et al. (2018). High-resolution μCT of a mouse embryo using a compact laser-driven X-ray betatron source. Proc. Natl. Acad. Sci. USA *115*, 6335–6340. https://doi.org/10.1073/pnas.1802314115.

14. Wong, M.D., Dorr, A.E., Walls, J.R., Lerch, J.P., and Henkelman, R.M. (2012). A novel 3D mouse embryo atlas based on micro-CT. Development *139*, 3248–3256. https://doi.org/10.1242/dev.082016.

15. Schneider, J.E., Böse, J., Bamforth, S.D., Gruber, A.D., Broadbent, C., Clarke, K., Neubauer, S., Lengeling, A., and Bhattacharya, S. (2004). Identification of cardiac malformations in mice lacking Ptdsr using a novel high-throughput magnetic

resonance imaging technique. BMC Dev. Biol. *4*, 16. https://doi.org/10.1186/1471-213X-4-16.

16. Lee, S.H., Han, M.J., Lee, J., and Lee, S.K. (2020). Experimental setup for bulk susceptibility effect-minimized, multi-orientation MRI of ex vivo tissue samples. Med. Phys. *47*, 3032–3043. https://doi.org/10.1002/mp.14174.

17. Scheffler, M., Maturana, E., Salomir, R., Haller, S., and Kövari, E. (2018). Air bubble artifact reduction in post-mortem whole-brain MRI: the influence of receiver bandwidth. Neuroradiology *60*, 1089–1092. https://doi.org/10.1007/s00234-018-2071-8.

18. Iglesias, J.E., Crampsie, S., Strand, C., Tachrount, M., Thomas, D.L., and Holton, J.L. (2018). Effect of Fluorinert on the histological Properties of formalin-fixed human brain tissue. J. Neuropathol. Exp. Neurol. *77*, 1085–1090. https://doi.org/10.1093/jnen/nly098.

19. Shatil, A.S., Matsuda, K.M., and Figley, C.R. (2016). A method for whole brain ex vivo magnetic resonance imaging with minimal susceptibility artifacts. Front. Neurol. *7*, 208. https://doi.org/10.3389/fneur.2016.00208.

20. Johnston, F.B., Urbas, B., and Khanzada, G. (1968). Effect of storage on the size distribution and amylose/amylopectin ratio in potato starch granules. Am. Potato J. *45*, 315–321.

21. Tang, H., Mitsunaga, T., and Kawamura, Y. (2006). Molecular arrangement in blocklets and starch granule architecture. Carbohydr. Polym. *63*, 555–560.

22. Clavaud, C., Bérut, A., Metzger, B., and Forterre, Y. (2017). Revealing the frictional transition in shear-thickening suspensions. Proc. Natl. Acad. Sci. USA *114*, 5147–5152. https://doi.org/10.1073/pnas.1703926114.

23. Zhu, F. (2017). NMR spectroscopy of starch systems. Food Hydrocolloids *63*, 611–624.

24. Larrea-Wachtendorff, D., Del Grosso, V., and Ferrari, G. (2022). Evaluation of the Physical stability of starch-based hydrogels Produced by high-pressure processing (HPP). Gels *8*, 152. https://doi.org/10.3390/gels8030152.

25. Ritota, M., Gianferri, R., Bucci, R., and Brosio, E. (2008). Proton NMR relaxation study of swelling and gelatinisation process in rice starch-water samples. Food Chem. *110*, 14–22. https://doi.org/10.1016/j.foodchem.2008.01.048.

26. Luo, H., Guo, C., Lin, L., Si, Y., Gao, X., Xu, D., Jia, R., and Yang, W. (2020). Combined use of rheology, LF-NMR, and MRI for characterizing the gel Properties of hairtail surimi with potato starch. Food Bioproc. Tech. *13*, 637–647. https://doi.org/10.1007/s11947-020-02423-y.

27. Witek, M., Peemoeller, H., Szymońska, J., and Blicharska, B. (2006). Investigation o f starch hydration by 2D time domain NMR. Acta Phys. Pol. A *109*, 359–364.

28. Tsurugizawa, T., Tamada, K., Ono, N., Karakawa, S., Kodama, Y., Debacker, C., Hata, J., Okano, H., Kitamura, A., Zalesky, A., and Takumi, T. (2020). Awake functional MRI detects neural circuit dysfunction in a mouse model of autism. Sci. Adv. *6*, eaav4520. https://doi.org/10.1126/sciadv.aav4520.

29. Zhang, J., Jones, M.V., McMahon, M.T., Mori, S., and Calabresi, P.A. (2012). In vivo and ex vivo diffusion tensor imaging of cuprizone-induced demyelination in the mouse corpus callosum. Magn. Reson. Med. *67*, 750–759. https://doi.org/10.1002/mrm.23032.

30. Cohen, O., and Ackerman, J.L. (2018). Ex vivo mouse brain microscopy at 15T with loop-gap RF coil. Magn. Reson. Imaging *51*, 1–6. https://doi.org/10.1016/j.mri.2018.04.010.

31. Yates, N.J., Feindel, K.W., Mehnert, A., Beare, R., Quick, S., Blache, D., Pillow, J.J., and Hunt, R.W. (2020). Ex vivo MRI analytical methods and brain Pathology in Preterm lambs treated with Postnatal dexamethasone (dagger). Brain Sci. *10*, 211. https://doi.org/10.3390/brainsci10040211.

32. Sjöqvist, M., and Gatenholm, P. (2005). The effect of starch composition on structure of foams prepared by microwave treatment. J. Polym. Environ. *13*, 29–37.

33. Rorden, C., Karnath, H.O., and Bonilha, L. (2007). Improving lesion-symptom mapping. J. Cogn. Neurosci. *19*, 1081–1088. https://doi.org/10.1162/jocn.2007.19.7.1081.

STAR★METHODS

KEY RESOURCES TABLE

REAGENT or RESOURCE	SOURCE	IDENTIFIER
Biological samples		
Two *ex vivo* embryos of a C57BL/6J mouse removed from the placenta of the mother mouse at embryo day 16 (E16).	This paper	N/A
Chemicals, peptides, and recombinant proteins		
Paraformaldehyde	FUJIFILM	Cat# 163-20145
Phosphate buffered saline	Takara	Cat# T9181
sodium azide	Nacalai	Cas# 26628-22-8
Gadoteridol	Eisai Co., Ltd.	Cas# 120066-54-8
FC43	3M Japan	Cat# 414-9547-329
Potate starch	Merck	Cat# 28-4960-5-500G-J
Software and algorithms		
MATLAB (2021b)	Mathworks	http://www.mathworks.com/products/matlab/
SPM12	The Wellcome Centre for Human Neuroimaging	https://www.fil.ion.ucl.ac.uk/spm/software/spm12/

RESOURCE AVAILABILITY

Lead contact

Further information about the methods and requests for data or scripts should be directed to and will be fulfilled by the lead contact, Tomokazu Tsurugizawa (t-tsurugizawa@aist.go.jp).

Materials availability

No materials were generated in this study that need to be made available. This study did not generate new unique reagents.

Data and code availability

No new code was used in this study. Any additional information regarding data or data analysis reported in this paper can be available from the lead contact upon request.

EXPERIMENTAL MODELS AND SUBJECT DETAILS

Animals

The fixation of mouse embryos was performed at the Tokyo Metropolitan Institute of Medical Science. The animal was treated following the Tokyo Metropolitan Institute of Medical Science Animals Care and Use Committee guidelines. Two embryos of male C57BL/6J mouse were removed from the placenta of the mother mouse at embryo day 16 (E16); one is used for Gd-contrast and another is used without Gd. The whole body of the removed embryo was fixed with 4% paraformaldehyde (PFA) at 4 °C until the imaging. At least three days before imaging, the embryo was washed three times with PBS and then transferred into PBS containing 0.1% sodium azide. The embryo's whole body was immersed in a 5 mM Gd (Gadoteridol, Eisai Co., Ltd., Japan) solution, which was solved in PBS for more than 1 week, for the Gd-contrast embryo.

METHOD DETAILS

Sample preparation

Following Gd penetration, the mouse embryo was sequentially imaged with Gd-PBS, FC43 (Fluorinert, 3M Japan Co., Ltd., Japan), or Gd-PS-PBS. The PBS, FC43, and PS-PBS were used as surrounding liquid for the PBS incubation embryo. The sequence of surrounding liquid was randomly determined, and the embryo was washed by PBS for PBS-incubated embryo or washed by Gd-PBS for Gd-penetrated embryo when

changing the surrounding liquid. During the MRI scanning of the mouse embryo with PBS, Gd-PBS, or FC43, the whole body of the embryo was fixed using the sponge only or sponge + plastic block (Figure 1A). The sponge and the plastic block were confirmed to tightly prevent the movement of the embryo by the eyes. For MRI scanning with PS-PBS, the mouse embryo was firstly immersed in PBS for the potato starch experiment and then the same volume of PS was gradually added into PBS. At room temperature, PS was not solved in the water but diffused into the water. After 10 min following the addition of the same volume of PS into the embryo in PS, the PS suspension was stable and the residual (Gd-)PBS was on the (Gd-)PS-PBS. We confirmed that the ratio of PS and (Gd-)PBS (v/v) in PS suspension was 2:1 (Figure S4). PS-PBS and Gd-PS-PBS were made by the same protocol as the embryo experiment for T1 and T2 relaxation time measurement.

T1 and T2 relaxation time measurement

All MRI acquisition was conducted at Bruker 11.7 T vertical magnet with a volume coil (Bruker BioSpin, Ettlingen, Germany). A longitudinal relaxation time (T1) of each material (PBS, Gd-PBS, PS power, PS-PBS, and Gd-PS-PBS) was calculated using rapid acquisition using relaxation enhancement (RARE) with variable TR pulse (RARE-VTR) sequence with the following parameters: TR = 40, 80, 150, 300, 600, 1250, 2,500, 5,000 ms, TE = 12 ms, spatial resolution = 195 × 195 μm^2/pixel, slice thickness = 570 μm, and 1 slice. A vertical relaxation time (T2) was calculated using a multi-slice multi-echo (MSME) sequence with the following parameters: TR = 2500 ms, TE = 100, 200, 300, 400, 500, 600, 700, 800, 900, 1,000, 1,100, 1,200, 1300, 1,400, 1,500, 1,600 ms, spatial resolution = 195 × 195 μm^2/voxel, slice thickness = 570 μm, and 1 slice.

T1-and T2-weighted images of mouse embryos

The T1 images of the mouse embryo were acquired by fast low-angle shot (FLASH) with the following parameters: TE/TR = 4/60 ms, spatial resolution = 78.1 × 78.1 μm^2/voxel, slice thickness = 0.8 mm, 4 slices. The T2 images of the mouse embryo were acquired by RARE with the following parameters: effective TE/TR = 46.9/5,000 ms, spatial resolution = 78.1 × 78.1 μm^2/pixel, slice thickness = 0.5 mm, RARE factor = 16, and 12 slices. The ultrahigh-resolution image of a Gd-penetrated embryo with Gd-PS-PBS were acquired using three-dimensional FLASH with the following parameters: TE/TR: 6/40 ms, field of view = 15.0 × 15.0 × 9.0 mm^3, spatial resolution = 29 × 29 × 50 μm^3/voxel, FA: 90°, 8 averages, and total scan time = 8 h 11 m and 31 s. For the assessment of the body movement, following parameters were used with 10 repetition, TE/TR = 4/300 ms, spatial resolution = 78.1 × 78.1 μm^2/voxel, slice thickness = 0.2 mm, 20 slices, 5 averages for FLASH and TE/TR = 46.9/5,000 ms, spatial resolution = 78.1 × 78.1 μm^2/pixel, slice thickness = 0.2 mm, rare factor = 16, and 12 slices for RARE.

Image processing

Parametric T1 and T2 relaxation time was calculated from the averaged signal intensities within ROIs, which were drawn using MRIcron.[33] The theoretical expression of T1 and signal intensity is: $SI = M_0 * (1 - \exp[-TR/T1])$, where SI is signal intensity, TR is repetition time, and M_0 is maximum longitudinal signal intensity. The theoretical expression of T2 and signal intensity is $SI = PD * \exp(-TE/T2)$, where TE is echo time and PD is a proton density. The body movement of the embryo was investigated using the realignment processing program of SPM12 (The Wellcome Center for Human Neuroimaging, London, UK). The six motion parameters, including the three translations and three rotations across orthogonal axis, were calculated.

QUANTIFICATION AND STATISTICAL ANALYSES

This study compared the T1, T2 and image quality of PS, FC43, and saline. The statistical analysis was not be performed.